Fully Dynamic 2D Two-Link Walker Simulation

MEGN505 — Advanced Dynamics

Ceja Florendo & Brayden Wilsey

8/14/2025

Abstract

We built a 2D bipedal walking simulation, including two legs (one hip and knee angle per leg) and a point-mass hip that was constrained to horizontal motion. We derived the leg equations in standard robot form and modeled ground reaction forces with a very stiff (40,000 N/m) vertical spring. In the horizontal direction, we used a Coulomb-capped tangential force with added damping to further limit slip. The joint motion tracks sinusoidal references via PD control, and the forward speed is regulated by commanding the stance foot to push the hip toward the target velocity. In the simulation, the walker begins gait and quickly reaches the target speed. Joint trajectories repeat each step, with force inputs from the controller to maintain the target speed. After obtaining a stable walker, we tested the model's sensitivity to perturbations in various ICs, such as friction and control gains.

1. Motivation

We wanted to build a 'from-scratch' simplified walking model that we could actually understand and tune. With backgrounds in biomechanics, we have both extensively used OpenSim and have had some exposure to the inner workings but felt that this project would be a good opportunity to better understand the techniques used now that we have formally learned the important dynamics concepts. A simple model like this makes it easier to see how joint torques, foot contact, and timing create motion and is free of the complexity of the giant state space that comes with more complex models. Passive dynamic walkers and the "simplest walking model" showed that gaits can emerge with little or no actuation [1, 2]. We wanted to keep our model to a similar complexity but add light controls so that we could practice applying the ideas from this class in a controls context. Our model is way simpler than full ZMP/preview-control robots [3], but we were still able to achieve a similar stable gait cycle. It also lines up with the hybrid view of walking (contact on/off) that shows up in HZD-style analysis [4]. For contact, we again tried to simplify it as much as possible but realize there are better methods that will be touched on later [5, 6].

2. Model Components

2.1 States and geometry

We track

$$\mathbf{q} = \begin{bmatrix} x_{\text{hip}} \\ \theta_L \\ \delta_L \\ \theta_R \\ \delta_R \end{bmatrix}, \quad \dot{\mathbf{q}} = \begin{bmatrix} \dot{x}_{\text{hip}} \\ \dot{\theta}_L \\ \dot{\delta}_L \\ \dot{\theta}_R \\ \dot{\delta}_R \end{bmatrix}.$$

The hip height h_{hip} is fixed for simplicity. θ is the thigh angle from vertical and δ is the knee flexion, so the total shank angle is $\theta + \delta$. Segment lengths are L_1 (thigh) and L_2 (shank). Each leg has a point mass at its distal end and the hip is a point mass that is restricted to translate only in x.

2.2 Foot kinematics

For one leg with angles θ, δ:

$$\begin{aligned}
x_f &= x_{\text{hip}} + L_1 \sin\theta + L_2 \sin(\theta + \delta), \\
y_f &= h_{\text{hip}} - L_1 \cos\theta - L_2 \cos(\theta + \delta), \\
\dot{x}_f &= \dot{x}_{\text{hip}} + L_1 \cos\theta\, \dot{\theta} + L_2 \cos(\theta + \delta)\, (\dot{\theta} + \dot{\delta}), \\
\dot{y}_f &= L_1 \sin\theta\, \dot{\theta} + L_2 \sin(\theta + \delta)\, (\dot{\theta} + \dot{\delta}).
\end{aligned}$$

We mapped foot forces to joint torques with the standard Jacobians $\mathbf{J}_x$ and $\mathbf{J}_y$ w.r.t. $[\theta\ \delta]^T$.

2.3 Dynamics

Each leg follows

$$\boxed{\mathbf{M}(\mathbf{q}_\ell)\, \ddot{\mathbf{q}}_\ell + \mathbf{C}(\mathbf{q}_\ell, \dot{\mathbf{q}}_\ell)\, \dot{\mathbf{q}}_\ell + \mathbf{G}(\mathbf{q}_\ell) = \tau_\ell + \mathbf{J}^\top(\mathbf{q}_\ell)\, \mathbf{F}}$$

with $\mathbf{q}_\ell = [\theta\ \delta]^T$, joint torques τ_ℓ, foot force $\mathbf{F} = [F_x \quad F_y]^T$, and $\mathbf{J}$ stacking $\mathbf{J}_x$ and $\mathbf{J}_y$. This is the same two-link structure used in many robot arm examples. The hip is described by:

$$\boxed{m_{\text{hip}}\, \ddot{x}_{\text{hip}} = F_{x,L} + F_{x,R}.}$$

Expanded Coefficients Let the leg coordinates be $\mathbf{q}_\ell = [\theta \quad \delta]^T$, where θ is the thigh angle (from vertical) and δ is the knee flexion; the total shank angle is $\theta + \delta$. With point masses m_{th} (thigh distal) and m_{sh} (shank distal), segment lengths L_1, L_2, and gravity g, the final coefficient matrices used in simulation are shown below. A full derivation can be found in Appendix A.

$$\mathbf{M}(\mathbf{q}_\ell) = \begin{bmatrix} (m_{\text{th}} + m_{\text{sh}})L_1^2 + m_{\text{sh}}L_2^2 + 2\, m_{\text{sh}}L_1L_2\, \cos(\delta) & m_{\text{sh}}L_2^2 + m_{\text{sh}}L_1L_2\, \cos(\delta) \\ m_{\text{sh}}L_2^2 + m_{\text{sh}}L_1L_2\, \cos(\delta) & m_{\text{sh}}L_2^2 \end{bmatrix}.$$

$$\mathbf{C}(\mathbf{q}_\ell, \dot{\mathbf{q}}_\ell) = \begin{bmatrix} -\, m_{\text{sh}} L_1 L_2 \, \sin(\delta)\, (\dot\theta + \dot\delta) & -\, m_{\text{sh}} L_1 L_2 \, \sin(\delta)\, \big(2\dot\theta + \dot\delta\big) \\ m_{\text{sh}} L_1 L_2 \, \sin(\delta)\, \dot\theta & 0 \end{bmatrix}, \qquad \text{used as } \mathbf{C} \begin{bmatrix} \dot\theta \\ \dot\theta + \dot\delta \end{bmatrix},$$

$$\mathbf{G}(\mathbf{q}_\ell) = \begin{bmatrix} (m_{\text{th}} + m_{\text{sh}})\, g\, L_1 \sin(\theta) + m_{\text{sh}}\, g\, L_2 \sin(\theta + \delta) \\ m_{\text{sh}}\, g\, L_2 \sin(\theta + \delta) \end{bmatrix},$$

$$\mathbf{J}_x(\mathbf{q}_\ell) = \begin{bmatrix} L_1 \cos(\theta) + L_2 \cos(\theta + \delta) \\ L_2 \cos(\theta + \delta) \end{bmatrix}, \qquad \mathbf{J}_y(\mathbf{q}_\ell) = \begin{bmatrix} L_1 \sin(\theta) + L_2 \sin(\theta + \delta) \\ L_2 \sin(\theta + \delta) \end{bmatrix}, \qquad \mathbf{J} = \begin{bmatrix} \mathbf{J}_x^\top \\ \mathbf{J}_y^\top \end{bmatrix}.$$

Reasoning for Approach We assumed that using: $M(q)\ddot{q} + C(q, \dot{q})\dot{q} + G(q) = \tau + J^\top F$ would be the most efficient method of expressing the dynamics of the system that we have learned in this class. We chose this because we could just model the ground contact and PD torques as non-conservative generalized forces via $J^\top F$. Then since the hip's horizontal DOF is so simple, we elected to just take a Newtonian approach: $m_{\text{hip}} \ddot{x}_{\text{hip}} = F_{x,L} + F_{x,R}$.

2.4 Contact and stance

Normal force. The ground only pushes up. If the foot is below the ground line ($y_f < 0$), we apply a spring force where k_{ground} is extremely high ($\approx 40\,000\,\frac{\text{N}}{\text{m}}$):

$$F_y = \begin{cases} k_{\text{ground}}\,(-y_f), & y_f < 0, \\ 0, & y_f \geq 0\ . \end{cases}$$

We kept this penalty model because it let us run `ode45` stably while keeping penetration small enough for our tests.

Friction The stance foot tries to push the hip toward the target speed. We compute a requested horizontal force and cap it by Coulomb friction:

$$F_x^{\text{req}} = K_{p,v}\big(v_{\text{des}} - \dot{x}_{\text{hip}}\big) - c_t\, \dot{x}_f,$$

$$F_x = \begin{cases} 0, & F_y \leq 0, \\ -\mu F_y, & F_x^{\text{req}} < -\mu F_y, \\ F_x^{\text{req}}, & |F_x^{\text{req}}| \leq \mu F_y, \\ +\mu F_y, & F_x^{\text{req}} > \mu F_y\ . \end{cases}$$

Where μ is the friction coefficient and c_t is tangential damping to reduce the little slips. In practice we saw early slip without the damping term, so we kept a modest c_t and used the Coulomb cap exactly as written.

Determining stance/swing cycle: We chose to alternate stance/swing with a simple clock $s(t) = \sin(\omega t)$ where $s < 0$ means left stance and $s \geq 0$ means right stance.

3. PD Controller

Joint PD. We track references with

$$\boxed{\tau = K_p(q_d - q) + K_d(\dot{q}_d - \dot{q}).}$$

Hip references are sinusoids with a π phase shift so the legs alternate. Knees flex only during swing using a smooth, gated sinusoid based on $s(t)$. We compute $\dot{q}_d$ analytically.

Hip speed. We set a desired speed v_{des} and let the stance foot supply horizontal force (limited by friction) to push the hip toward that target. For our goals, this minimalist setup was enough to hit the target speed without needing model-based feedforward.

4. IC's

Geometry/physics: $L_1 = 0.4\,\text{m}$, $L_2 = 0.3\,\text{m}$, $h_{\text{hip}} = 0.69\,\text{m}$, $m_{\text{hip}} = 20\,\text{kg}$, $m_{\text{th}} = 1\,\text{kg}$, $m_{\text{sh}} = 1\,\text{kg}$, $g = 9.81\,\text{m/s}^2$. We picked these values as they are relatively accurate to average anthropometry. The one notable value here is the $h_{\text{hip}} = 0.69\,\text{m}$ hip height. This was intentional to essentially start the model with its feet $h_{\text{hip}} = 0.01\,\text{m}$ below the ground so the GRF engages immediately without needing to include a pre-loading function.

Control: $K_p = 50$, $K_d = 5$, hip amplitude $\theta_{\text{amp}} = \pi/9$, knee amplitude $\delta_{\text{amp}} = \pi/6$, stride $f = 1\,\text{Hz}$ ($\omega = 2\pi f$). These values were good for steady walking but can be raised or lowered to speed up or slow down the simulation as desired (within reason).

Contact: $k_{\text{ground}} = 40.000\,\text{N/m}$, $\mu = 0.8$, $c_t = 80\,\text{N s/m}$. Like many of the other ICs, we settled on these values purely through trial and error. We found that any significant increases in ground stiffness didn't work well with our approach of starting the foot $-0.01\,\text{m}$ below the ground as it would just launch that foot. Also, since our slipping problem was so severe initially, we found a high CoF and damping coefficient to be necessary, especially to prevent slipping in the ramping phase of the hip velocity when the PD-induced joint torques are highest.

Speed target: $v_{\text{des}} = 0.3\,\text{m/s}$, $K_{p,v} = 120$. Again, these values were just what we found to yield the most stable baseline simulation through trial and error. One major constraint though on the velocity IC in particular is that slipping will occur if it is set too high and the PD controller forces joint torques too high for our no-slip constraints. This prevents the model from being an effective running simulator and we believe it yields the best results if $v_{\text{des}} < 0.5\,\text{m/s}$.

Integration: We used `ode45` like normal to generate the forward dynamics and set the tolerances to: `RelTol` $= 10^{-6}$, `AbsTol` $= 10^{-8}$, $t = [0, 10]$ s. Hip position, hip velocity, foot velocities, and joint angles were all integrated and plotted.

5. Results

5.1 Base Simulation Behavior

The hip moves at the right speed. After a short start-up, $x_{\text{hip}}(t)$ grows almost linearly. The average speed is close to v_{des}. There's a small step-to-step ripple because the friction cap changes the effective push during each stance.

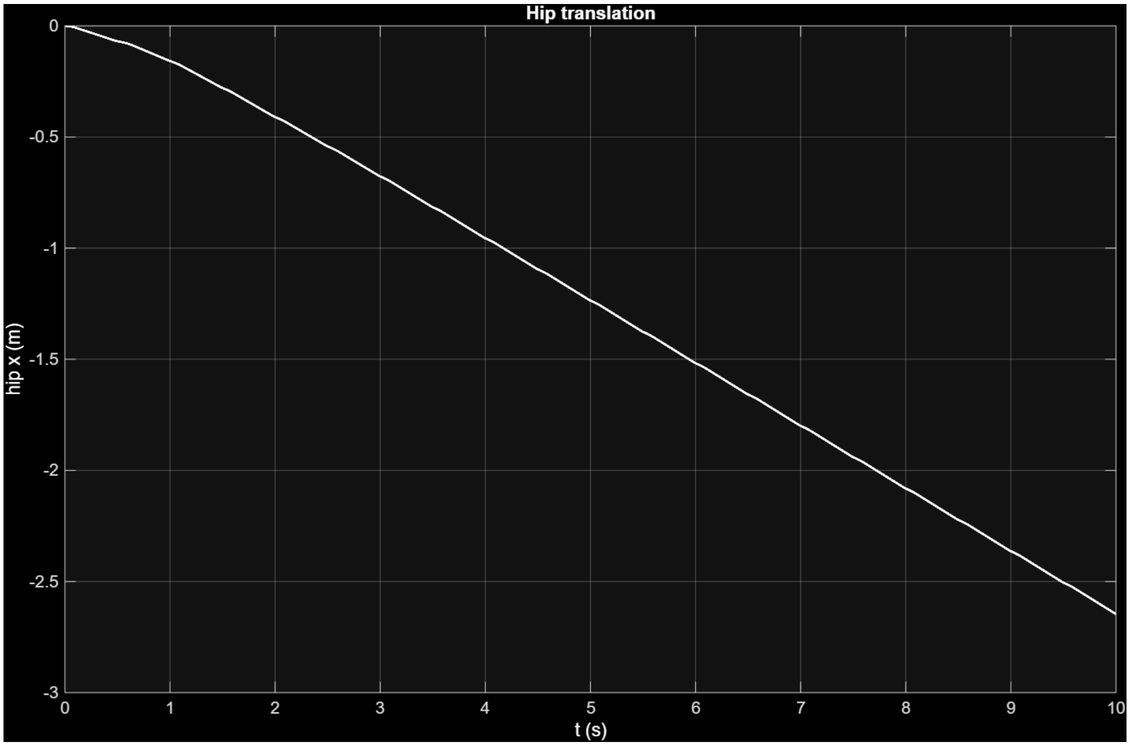

Figure 1: Hip position $x_{\text{hip}}(t)$ over time.

Effective no-slip conditions + cyclic motion. During stance, $\dot{x}_f \approx 0$ while the normal force is positive, so slip is small. During swing, the foot moves backward relative to the hip and then forward again to set up the next step. The vertical foot motion is a single clean arc per swing. The swing knee flexes and extends smoothly. With our chosen K_p and K_d this behavior is shown in the plots below:

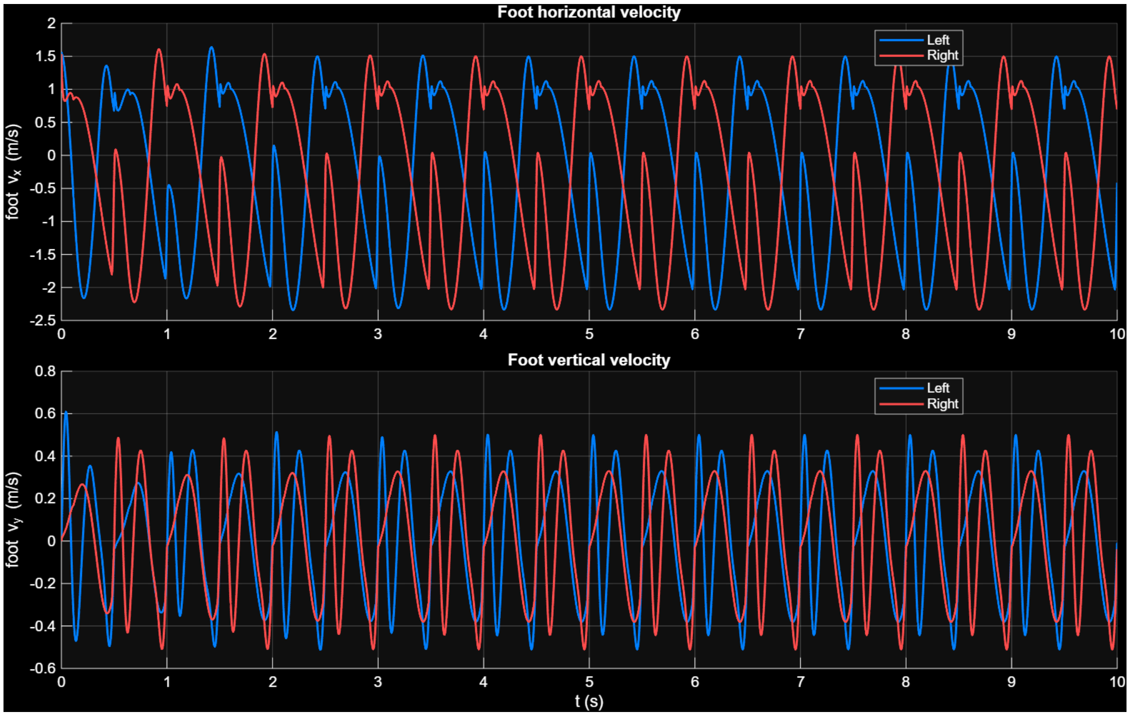

Figure 2: Foot velocity progression over a 10 s walking cycle. Noticeable stabilization once the controller reaches the target velocity.

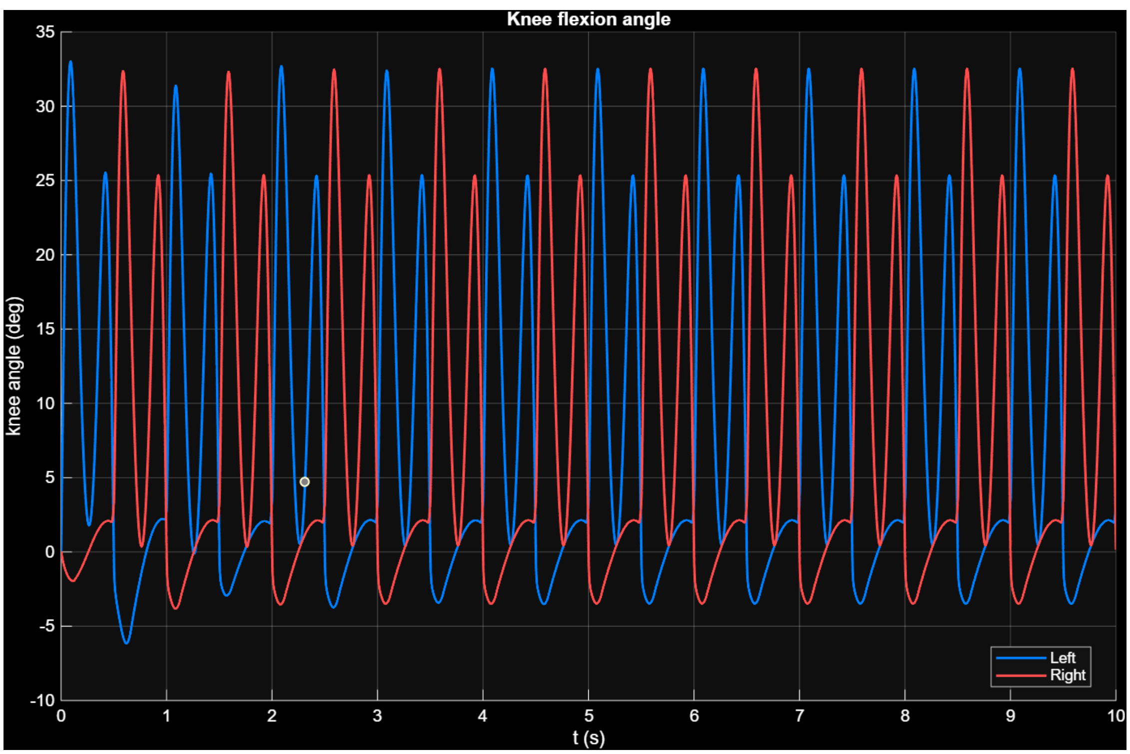

Figure 3: Knee angle progression over a 10 s walking cycle.

5.2 Effects of IC perturbations

Slippery patch: μ drops from 0.8 to 0.3 momentarily. We dropped friction to 0.3 for $t \in [4, 6]$ s (gray band). We aren't entirely sure how to explain the behavior, but our best guess is the stance foot slid backward, so the hip was pulled forward more than usual. Our controller also adds push when the foot slides ($-c_t\,\dot{x}_f$ term), so the model covered extra distance during the patch. When friction returned, speed matched baseline again, but the slip trial kept the lead.

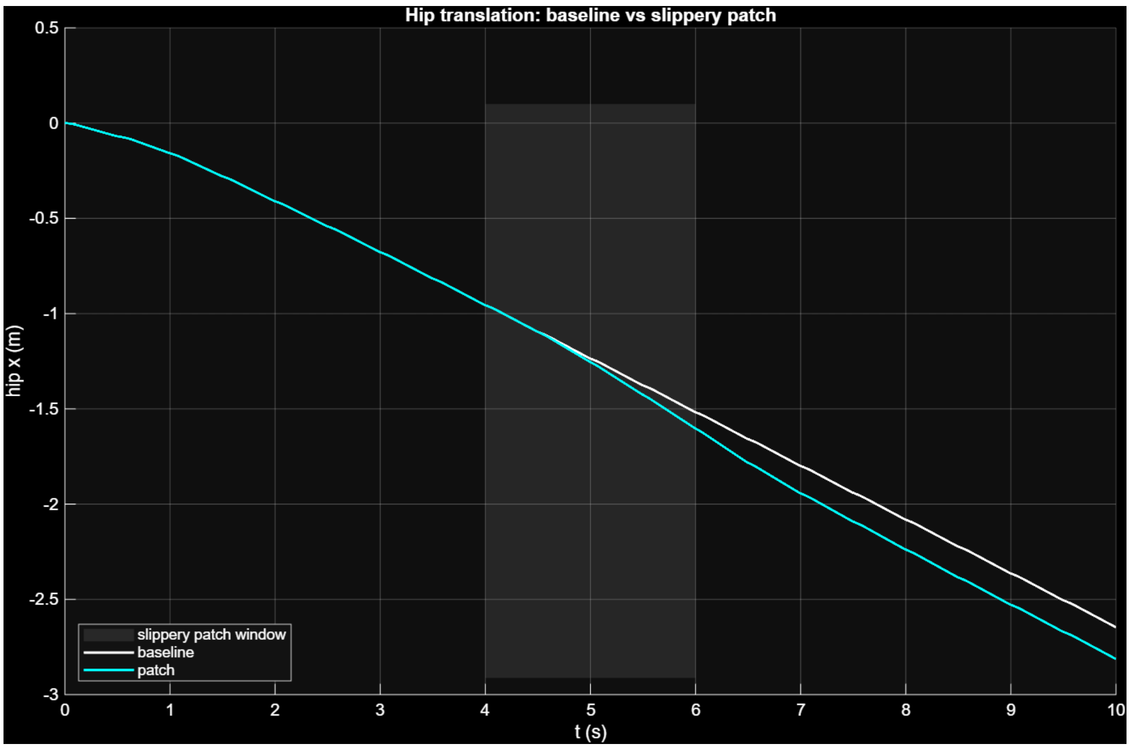

Figure 4: Hip translation with a 2 s CoF drop (μ from 0.8 to 0.3, $t \in [4, 6]$ s).

Increasing hip-speed gain $K_{p,v}$ (120 to 300). Raising $K_{p,v}$ can tighten speed tracking, but with limited friction it just pushes the controller into the Coulomb cap $|F_x| \leq \mu F_y$ more often. In the plot below, the hip-translation slope is nearly an order of magnitude smaller than the baseline. The high gain keeps F_x^{req} saturated and the tangential damper absorbs any small slips, so the walker basically walks in place. The foot velocity and knee angle plots remained the same as the baseline case.

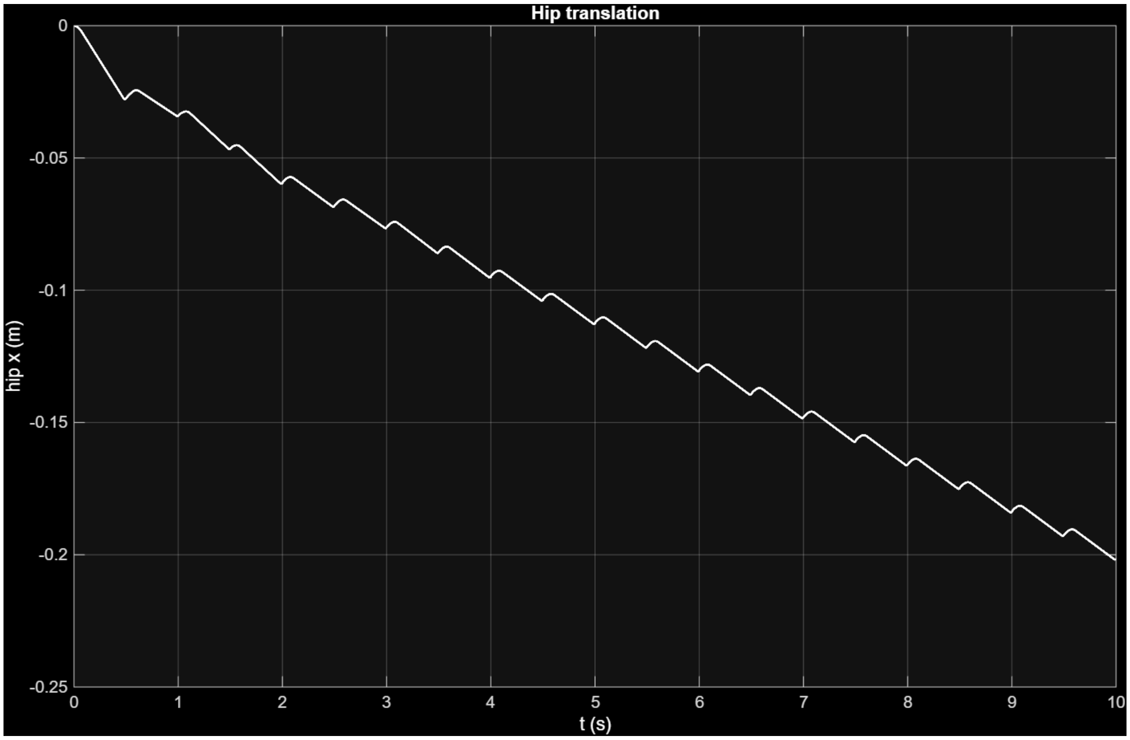

Figure 5: Hip translation with $K_{p,v} = 300$.

6. Assumptions

2D w/ fixed hip height We always intended to keep the model 2D, but found out once we started working on it that limiting the PD controller to only controlling velocity in the x rather than both x and y was much easier and we did this by fixing the hip height. This let us focus on generating the correct motion without all the added complexity of free upper segments. It does severely simplify the model though. The vertical translation of the hip is extremely important in gait, and you can see this manifest in the simulation as the walker can only take very small steps.

Lumped masses This helped simplify the math a ton but if the goal of the simulation was realistic energy analysis then this assumption would no longer be valid. Since the model is only intended to operate slowly and we aren't concerned with realistic energies, this does not affect the validity of our results.

Penalty contact The GRF spring was easy and works with `ode45`, but it does allow for small penetration and needed tuning. For a more realistic approach (and what tends to be done in papers we referenced), we'd switch to rigid contact with a complementarity or implicit time-stepping method to get proper stick/slide and impact handling [5, 6].

Time-based stance switching Using $s(t)$ worked well for our purposes, but realistically, gait timing can drift. A better approach is switching on actual touchdown ($y_f = 0$) and applying an inelastic impact, which also plugs into hybrid limit-cycle tools [4].

7. Takeaways

What worked. We were pleased with the success of the underlying equations, which was really the important part concerning this class. Using the M–C–G structure and $J^\top F$ was definitely the right approach and makes it clear how foot forces show up as joint torques. Even though many of the constraints on the system were modeled in the most simple way we could find, we found this to be stable enough within the range of ICs we wanted the system to operate in.

What surprised us. There were many quirks that arose in the creation of the model but they were interesting nonetheless. Some examples of these are if friction is low or $K_{p,v}$ is high, the push from the PD controller hits the friction cap and slip shows up quickly and the gait destabilizes. Also, very stiff ground can make vertical oscillations appear as there is no control in the y. There were also some cases where the gait clock hits an edge case and we see things like a double step or a no-step which were certainly interesting to watch.

Skills we practiced. This project ended up being pretty intensive. From coming up with generalized coordinates, developing the coefficients for the robot equations, coupling contact with $J^\top F$, and designing simple PD and a speed regulator was a far stretch of the skills we learned in this class. We agree that in working through all these issues and figuring out how to apply what we've learned in the context of a problem that we were allowed to parameterize was so helpful in actually understanding the material. We realize that we made a ton of simplifications, even with things that we technically could've done with our current knowledge, particularly not treating the segments as rigid bodies, but even still this project felt like a very solid application of all the topics covered in this class.

8. Conclusion + Future Work

We successfully built a fully dynamic, simplified 2D walker with PD joint control and a friction-induced "push" to induce gait at a set speed on flat ground. The simulation is stable within a reasonable range of ICs and is easy to modify to analyze the effects of various changes on the model. With more time, the next steps would be to use the more literature-standard approaches for various things like:

- switch stance on actual touchdown and include an impact map
- move to a more physical contact solver
- add vertical hip motion
- treat segments as rigid bodies
- try preview/COM control to handle bumps or uneven terrain [3, 4]
- explore further perturbations with a more realistic model

Appendix A: Derivation of $\mathbf{M}, \mathbf{C}, \mathbf{G}$ and $\mathbf{J}$

Kinematics. Knee and foot positions:

$$x_k = L_1 \sin\theta, \quad y_k = h_{\text{hip}} - L_1 \cos\theta, \qquad x_f = L_1 \sin\theta + L_2 \sin(\theta+\delta), \quad y_f = h_{\text{hip}} - L_1\cos\theta - L_2\cos(\theta+\delta).$$

Velocities:

$$\dot{x}_k = L_1 \cos\theta\,\dot{\theta}, \quad \dot{y}_k = L_1 \sin\theta\,\dot{\theta},$$
$$\dot{x}_f = L_1 \cos\theta\,\dot{\theta} + L_2\cos(\theta+\delta)(\dot{\theta}+\dot{\delta}), \quad \dot{y}_f = L_1 \sin\theta\,\dot{\theta} + L_2\sin(\theta+\delta)(\dot{\theta}+\dot{\delta}).$$

Jacobian From the foot position

$$x_f = L_1 \sin\theta + L_2\sin(\theta+\delta), \qquad y_f = h_{\text{hip}} - L_1\cos\theta - L_2\cos(\theta+\delta),$$

we take the partial derivatives w.r.t. $[\theta \;\; \delta]^T$:

$$\frac{\partial x_f}{\partial \theta} = L_1\cos\theta + L_2\cos(\theta+\delta), \qquad \frac{\partial x_f}{\partial \delta} = L_2\cos(\theta+\delta),$$
$$\frac{\partial y_f}{\partial \theta} = L_1\sin\theta + L_2\sin(\theta+\delta), \qquad \frac{\partial y_f}{\partial \delta} = L_2\sin(\theta+\delta).$$

Thus

$$\mathbf{J}(\mathbf{q}_\ell) = \begin{bmatrix} \dfrac{\partial x_f}{\partial \theta} & \dfrac{\partial x_f}{\partial \delta} \\ \dfrac{\partial y_f}{\partial \theta} & \dfrac{\partial y_f}{\partial \delta} \end{bmatrix} = \begin{bmatrix} L_1\cos\theta + L_2\cos(\theta+\delta) & L_2\cos(\theta+\delta) \\ L_1\sin\theta + L_2\sin(\theta+\delta) & L_2\sin(\theta+\delta) \end{bmatrix}.$$

In the code we broke the Jacobian into:

$$\mathbf{J}_x(\mathbf{q}_\ell) = \begin{bmatrix} L_1\cos\theta + L_2\cos(\theta+\delta) \\ L_2\cos(\theta+\delta) \end{bmatrix}, \qquad \mathbf{J}_y(\mathbf{q}_\ell) = \begin{bmatrix} L_1\sin\theta + L_2\sin(\theta+\delta) \\ L_2\sin(\theta+\delta) \end{bmatrix}, \qquad \mathbf{J} = \begin{bmatrix} \mathbf{J}_x^\top \\ \mathbf{J}_y^\top \end{bmatrix}.$$

Energies. Kinetic and potential energies:

$$T = \tfrac{1}{2} m_{\text{th}}\left(\dot{x}_k^2 + \dot{y}_k^2\right) + \tfrac{1}{2} m_{\text{sh}}\left(\dot{x}_f^2 + \dot{y}_f^2\right), \qquad V = -(m_{\text{th}} + m_{\text{sh}})\, g\, L_1\cos\theta - m_{\text{sh}}\, g\, L_2\cos(\theta+\delta) \ (+\text{const}).$$

Using $\cos(\theta+\delta)\cos\theta + \sin(\theta+\delta)\sin\theta = \cos\delta$, the foot speed simplifies to

$$\dot{x}_f^2 + \dot{y}_f^2 = L_1^2\dot{\theta}^2 + L_2^2(\dot{\theta}+\dot{\delta})^2 + 2L_1L_2\cos(\delta)\,\dot{\theta}(\dot{\theta}+\dot{\delta}),$$

so

$$T = \tfrac{1}{2}(m_{\text{th}} + m_{\text{sh}})L_1^2\dot{\theta}^2 + \tfrac{1}{2} m_{\text{sh}} L_2^2(\dot{\theta}+\dot{\delta})^2 + m_{\text{sh}} L_1 L_2 \cos(\delta)\,\dot{\theta}(\dot{\theta}+\dot{\delta}).$$

Lagrange's equations. Let $L = T - V$, $q_1 = \theta$, $q_2 = \delta$:

$$\frac{d}{dt}\Big(\frac{\partial L}{\partial \dot{q}_i}\Big) - \frac{\partial L}{\partial q_i} = Q_i, \qquad \mathbf{Q} = \tau_\ell + \mathbf{J}^\top \mathbf{F}.$$

Velocity partials:

$$\frac{\partial T}{\partial \dot{\theta}} = \big[(m_{\text{th}} + m_{\text{sh}})L_1^2 + m_{\text{sh}}L_2^2 + 2m_{\text{sh}}L_1L_2\cos\delta\big]\dot{\theta} + \big[m_{\text{sh}}L_2^2 + m_{\text{sh}}L_1L_2\cos\delta\big]\dot{\delta},$$

$$\frac{\partial T}{\partial \dot{\delta}} = \big[m_{\text{sh}}L_2^2 + m_{\text{sh}}L_1L_2\cos\delta\big]\dot{\theta} + \big[m_{\text{sh}}L_2^2\big]\dot{\delta}.$$

Time derivatives:

$$\frac{d}{dt}\left(\frac{\partial T}{\partial \dot{\theta}}\right) = M_{11}\ddot{\theta} + M_{12}\ddot{\delta} - \; m_{\text{sh}}L_1L_2\sin\delta\,\dot{\delta}\,(2\dot{\theta} + \dot{\delta}),$$

$$\frac{d}{dt}\left(\frac{\partial T}{\partial \dot{\delta}}\right) = M_{21}\ddot{\theta} + M_{22}\ddot{\delta} + \; m_{\text{sh}}L_1L_2\sin\delta\,\dot{\theta}^{\,2},$$

where

$M_{11} = (m_{\text{th}}+m_{\text{sh}})L_1^2+m_{\text{sh}}L_2^2+2m_{\text{sh}}L_1L_2\cos\delta, \quad M_{12} = M_{21} = m_{\text{sh}}L_2^2+m_{\text{sh}}L_1L_2\cos\delta, \quad M_{22} = m_{\text{sh}}L_2^2.$

Partials from V:

$$\frac{\partial V}{\partial \theta} = (m_{\text{th}} + m_{\text{sh}})\,g\,L_1\sin\theta + m_{\text{sh}}\,g\,L_2\sin(\theta+\delta), \qquad \frac{\partial V}{\partial \delta} = m_{\text{sh}}\,g\,L_2\sin(\theta+\delta).$$

Final forms. Grouping terms gives

$$\mathbf{M}(\mathbf{q}_\ell)\ddot{\mathbf{q}}_\ell + \mathbf{C}(\mathbf{q}_\ell, \dot{\mathbf{q}}_\ell)\dot{\mathbf{q}}_\ell + \mathbf{G}(\mathbf{q}_\ell) = \tau_\ell + \mathbf{J}^\top\mathbf{F},$$

with

$$\mathbf{M}(\mathbf{q}_\ell) = \begin{bmatrix} (m_{\text{th}} + m_{\text{sh}})L_1^2 + m_{\text{sh}}L_2^2 + 2\,m_{\text{sh}}L_1L_2\,\cos\delta & m_{\text{sh}}L_2^2 + m_{\text{sh}}L_1L_2\,\cos\delta \\ m_{\text{sh}}L_2^2 + m_{\text{sh}}L_1L_2\,\cos\delta & m_{\text{sh}}L_2^2 \end{bmatrix}.$$

$$\mathbf{C}(\mathbf{q}_\ell, \dot{\mathbf{q}}_\ell) = \begin{bmatrix} -\,m_{\text{sh}}L_1L_2\,\sin\delta\,(\dot{\theta} + \dot{\delta}) & -\,m_{\text{sh}}L_1L_2\,\sin\delta\,\big(2\dot{\theta} + \dot{\delta}\big) \\ m_{\text{sh}}L_1L_2\,\sin\delta\,\dot{\theta} & 0 \end{bmatrix}.$$

$$\mathbf{G}(\mathbf{q}_\ell) = \begin{bmatrix} (m_{\text{th}} + m_{\text{sh}})\,g\,L_1\sin\theta + m_{\text{sh}}\,g\,L_2\sin(\theta+\delta) \\ m_{\text{sh}}\,g\,L_2\sin(\theta+\delta) \end{bmatrix}.$$

Foot Jacobians

$$\mathbf{J}_x(\mathbf{q}_\ell) = \begin{bmatrix} L_1\cos\theta + L_2\cos(\theta+\delta) \\ L_2\cos(\theta+\delta) \end{bmatrix}, \qquad \mathbf{J}_y(\mathbf{q}_\ell) = \begin{bmatrix} L_1\sin\theta + L_2\sin(\theta+\delta) \\ L_2\sin(\theta+\delta) \end{bmatrix}, \qquad \mathbf{J} = \begin{bmatrix} \mathbf{J}_x^\top \\ \mathbf{J}_y^\top \end{bmatrix}.$$

References

[1] T. McGeer, "Passive dynamic walking," *International Journal of Robotics Research*, vol. 9, no. 2, pp. 62–82, 1990. doi: 10.1177/027836499000900206.

[2] M. Garcia, A. Chatterjee, A. Ruina, and M. Coleman, "The simplest walking model: Stability, complexity, and scaling," *ASME Journal of Biomechanical Engineering*, vol. 120, no. 2, pp. 281–288, Apr. 1998. doi: 10.1115/1.2798313.

[3] S. Kajita, F. Kanehiro, K. Kaneko, K. Fujiwara, K. Harada, K. Yokoi, and H. Hirukawa, "Biped walking pattern generation by using preview control of zero-moment point," in *Proc. IEEE Int. Conf. Robotics and Automation (ICRA)*, Taipei, Taiwan, Sep. 2003, pp. 1620–1626.

[4] E. R. Westervelt, J. W. Grizzle, C. Chevallereau, J. H. Choi, and B. Morris, *Feedback Control of Dynamic Bipedal Robot Locomotion.* Boca Raton, FL, USA: CRC Press, 2007.

[5] D. E. Stewart and J. C. Trinkle, "An implicit time-stepping scheme for rigid body dynamics with Coulomb friction," *International Journal for Numerical Methods in Engineering*, vol. 39, no. 15, pp. 2673–2691, Aug. 1996. doi: 10.1002/(SICI)1097-0207(19960815)39:15¡2673::AID-NME972¿3.0.CO;2-I.

[6] M. Anitescu and F. A. Potra, "Formulating dynamic multi-rigid-body contact problems with friction as solvable linear complementarity problems," *Nonlinear Dynamics*, vol. 14, pp. 231–247, Nov. 1997. doi: 10.1023/A:1008292328909.